Quantitative sum rule analysis of low-temperature spectral functions

Nathan P. M. Holt,* Paul M. Hohler,† and Ralf Rapp‡
Cyclotron Institute and Department of Physics & Astronomy, Texas A&M University, College Station, Texas 77843-3366, USA
(Dated: July 9, 2018)

We analyze QCD and Weinberg-type sum rules in a low-temperature pion gas using vector and axial-vector spectral functions following from the model-independent chiral-mixing scheme. Toward this end we employ recently constructed vacuum spectral functions with ground and first-excited states in both channels and a universal perturbative continuum; they quantitatively describe hadronic τ-decay data and satisfy vacuum sum rules. These features facilitate the implementation of chiral mixing without further assumptions, and lead to in-medium spectral functions which exhibit a mutual tendency of compensating resonance and dip structures, suggestive for an approach toward structureless distributions. In the sum rule analysis, we account for pion mass corrections, which turn out to be significant. While the Weinberg sum rules remain satisfied even at high temperatures, the numerical evaluation of the QCD sum rules for vector and axial-vector channels reveals significant deviations setting in for temperatures beyond $\sim$140 MeV, suggestive of additional physics beyond low-energy chiral pion dynamics.

PACS numbers: 11.55.Hx, 12.38.Mh, 11.30.Rd

I. INTRODUCTION

The Lagrangian of quantum chromodynamics (QCD) is invariant under the transformations described by the chiral symmetry group $SU_L(N_f)\times SU_R(N_f)$, where N_f is the number of light-quark flavors [1–4]. In vacuum and at low temperatures, this symmetry is spontaneously broken by a nonzero expectation value of the quark condensate, $\langle 0|\,\bar{q}q\,|0\rangle$. For isovector hadronic excitations, this manifests itself through a large splitting of the masses of the chiral partner mesons $\rho(770)$ and $a_1(1260)$ [5].

Chiral symmetry is believed to be restored at high temperatures and baryon densities. As with any symmetry, its breaking and restoration can be described by order parameters. For the chiral phase transition of QCD, the canonical order parameter is the quark condensate. Lattice-QCD computations have found that the quark condensate "melts" with increasing temperature [6, 7] until its disappearance signals the restoration of chiral symmetry. The gradual dissolution of the quark condensate is expected to be accompanied by an emerging degeneracy of chiral partner hadrons. Thus, the ρ and a_1 masses, or more generally, the pertinent vector and axial-vector spectral functions, should approach each other with rising temperature and finally become degenerate when chiral symmetry is restored.

The interplay between the temperature dependence of spectral functions and condensates can be analyzed using finite-temperature sum rules. These relate integrals over spectral distributions to an operator product expansion (OPE) which is expressed in terms of low-energy condensates. The most relevant sum rules for the present work are the QCD sum rules (QCDSRs) [8, 9] and the Weinberg-type sum rules (WSRs) [10–12]. The former are channel specific, i.e., they differ for the vector and axial-vector channels, and they contain both chirally breaking and symmetric operators. The latter relate moments of the difference between the vector and axial-vector spectral functions to chiral order parameters. Both sets of sum rules provide useful tools from which either the temperature dependence of the spectral functions can be constrained, or by which models of temperature dependence of the spectral functions and condensates can be tested [3].

A low-temperature medium at vanishing chemical potential can be represented by a dilute gas of thermally excited pions. In Ref. [13], it was shown that the pertinent in-medium vector and axial-vector spectral distributions can be deduced model-independently as linear combinations of the vacuum distributions, where the strength of the "mixing" is determined by thermal pion exchange (cf. also [14–17]). It was further noted that the mixing effect straightforwardly satisfies the WSRs, which has been verified subsequently [12, 18]. Conversely, the finite-temperature QCDSRs have not received much attention in the context of chiral mixing. Rather, the (low-) temperature dependence of the condensates has been evaluated and subsequently used to infer properties of vector and axial-vector spectral functions [19–21]. More recently, chirally mixed spectral functions have been implemented within so-called finite-energy sum rules (FESRs) which are obtained from moments of the QCDSRs [22, 23].

In the present work, we revisit the use of chirally mixed spectral functions in both WSRs and QCDSRs utilizing updated vacuum spectral functions [24] and numerically evaluating the consequences of finite pion mass corrections. Certain features of the vacuum spectral functions, such as their degenerate continuum in vector and ax-

*Electronic address: nathan.holt@physics.tamu.edu
†Electronic address: pmhohler@comp.tamu.edu
‡Electronic address: rapp@comp.tamu.edu

ialvector channels and quantitative agreement with τ-decay data [25, 26], as well QCDSRs and WSRs, will turn out to be important in a quantitative low-temperature analysis.

The remainder of this paper is organized as follows. In Sec. II, we recollect vacuum and finite-temperature sum rules and discuss the leading temperature dependence and pion-mass corrections of the OPE coefficients. In Sec. III, we construct the finite-temperature vector and axial-vector spectral functions and discuss their characteristics. In Sec. IV, we quantitatively evaluate the in-medium WSRs and QCDSRs employing the chirally mixed spectral functions. We conclude in Sec. V.

II. QCD AND WEINBERG-TYPE SUM RULES

We begin by briefly reviewing the vacuum QCDSRs and WSRs (Sec. II A) and their extension to finite temperature (Secs. II B and II C, respectively). More detailed accounts for the vacuum case can be found in the original works [8–12] and at finite temperature in Refs. [12, 19, 21, 27].

A. Vacuum sum rules

QCD sum rules utilize a dispersion relation to relate a spectral function to an operator product expansion. A commonly used form (for operators with dimension less than 6) reads

$$\frac{1}{\mathcal{M}^2}\int \frac{\rho(s)}{s}\, e^{-s/\mathcal{M}^2}\,\mathrm{d}s = c_0+\frac{c_1}{\mathcal{M}^2}+\frac{c_2}{\mathcal{M}^4}+\frac{c_3}{\mathcal{M}^6}+\ldots, \quad (1)$$

where $\rho(s)$ is the spectral function of a given channel – $\rho_V(s)$ in the vector and $\bar{\rho}_A(s) = \rho_A(s) + f_\pi^2\, s\, \delta(s-m_\pi^2)$ in the axial-vector channel where the bar indicates the inclusion of the pion pole. The ellipsis designates terms associated with operators of higher dimension. A Borel transformation has traded the space-like four-momentum $q^2 = -Q^2$ for the Borel mass $\mathcal{M}^2$. The coefficients appearing on the right-hand side involve various condensates. For each condensate, we work to leading order in the quark mass, m_q; that is, we consider the effects of each condensate but not any finite quark mass correction. In the vector and axial-vector channels, one has

$$\begin{aligned} c_0^V = c_0^A &= \frac{1}{8\pi^2}\left(1+\frac{\alpha_s}{\pi}\right) , \\ c_1^V = c_1^A &= -\frac{3}{8}(m_u^2+m_d^2) \approx 0 , \\ c_2^V = c_2^A &= \frac{1}{24}\langle\frac{\alpha_s}{\pi}G_{\mu\nu}^2\rangle + m_q\langle\bar{q}q\rangle , \\ c_3^V &= -\frac{56}{81}\pi\alpha_s\langle\mathcal{O}_4^V\rangle , \\ c_3^A &= \frac{88}{81}\pi\alpha_s\langle\mathcal{O}_4^A\rangle . \end{aligned} \quad (2)$$

The gluon and quark condensate are denoted by $\langle\frac{\alpha_s}{\pi}G_{\mu\nu}^2\rangle$ and $\langle\bar{q}q\rangle$, respectively, where m_q is the average current light-quark mass; $\langle\mathcal{O}_4^V\rangle$ and $\langle\mathcal{O}_4^A\rangle$ refer to the vector and axial-vector four-quark condensates. Note that the only difference between the vector and axial-vector channels is due to the chirally odd c_3 terms. The four-quark condensates may be written in a factorized form,

$$\langle\mathcal{O}_4^{V,A}\rangle = \kappa_{V,A}\,\langle\bar{q}q\rangle^2 , \quad (3)$$

where $\kappa_{V,A}$ is a parameter greater than one which accounts for the deviation from vacuum-state saturation. In principle, the values of κ need not be identical in the two channels as the four-quark operators are not identical. In Ref. [24], it was found that the QCDSRs in both channels can be satisfied with a single value for κ.

The vacuum WSRs are constructed from the moments of the difference of the vector and axial-vector spectral functions, denoted by $\Delta\rho(s) = \rho_V(s) - \rho_A(s)$. They read

$$\text{(WSR-0)} \qquad \int_0^\infty \frac{\Delta\rho(s)}{s^2}\,\mathrm{d}s = \frac{1}{3}f_\pi^2\,\langle r_\pi^2\rangle - F_A , \quad (4)$$

$$\text{(WSR-1)} \qquad \int_0^\infty \frac{\Delta\rho(s)}{s}\,\mathrm{d}s = f_\pi^2 , \quad (5)$$

$$\text{(WSR-2)} \qquad \int_0^\infty \Delta\rho(s)\,\mathrm{d}s = -2m_q\,\langle\bar{q}q\rangle = f_\pi^2 m_\pi^2 , \quad (6)$$

$$\text{(WSR-3)} \qquad \int_0^\infty \Delta\rho(s)\,s\,\mathrm{d}s = -2\pi\alpha_s\langle\mathcal{O}_4^{SB}\rangle . \quad (7)$$

Here, $\langle r_\pi^2\rangle$ is the average squared pion radius and F_A is the radiative pion decay constant. We have used the Gell-Mann-Oakes-Renner relation in WSR-2. The chiral order parameter appearing in WSR-3 is the chiral symmetry-breaking four-quark condensate and can be expressed in terms of the vector and axial-vector four-quark condensates as

$$\langle\mathcal{O}_4^{SB}\rangle = \frac{16}{9}\left(\frac{7}{18}\langle\mathcal{O}_4^V\rangle + \frac{11}{18}\langle\mathcal{O}_4^A\rangle\right). \quad (8)$$

This condensate can also be written in a factorized form as $\langle\mathcal{O}_4^{SB}\rangle = \frac{16}{9}\kappa\,\langle\bar{q}q\rangle^2$ with $\kappa = \frac{7}{18}\kappa_V + \frac{11}{18}\kappa_A$.

B. Finite temperature QCD sum rules

At finite temperatures, we will only consider mesons with vanishing three-momentum in the thermal rest frame. The finite-temperature QCDSRs then have the same structure as in Eq. (1) but with the condensates developing a temperature dependence and the appearance of additional nonscalar condensates [19]. The latter can be characterized by their twist, which is defined as the difference of an operator's dimension and its spin.

The finite-temperature c_2 and c_3 terms are then given by

$$c_2^{V/A}(T) = \frac{1}{24}\Big\langle\frac{\alpha_s}{\pi}G^2\Big\rangle_T + m_q\langle\bar{q}q\rangle_T + \big\langle\mathcal{O}^{\tau=2,s=2}\big\rangle_T\,, \quad (9)$$

$$c_3^V(T) = -\frac{56}{81}\pi\alpha_s\left\langle\mathcal{O}_4^V\right\rangle_T + \big\langle\mathcal{O}^{\tau=2,s=4}\big\rangle + \big\langle\mathcal{O}^{\tau=4,s=2}\big\rangle_T\,, \quad (10)$$

$$c_3^A(T) = \frac{88}{81}\pi\alpha_s\left\langle\mathcal{O}_4^A\right\rangle_T + \big\langle\mathcal{O}^{\tau=2,s=4}\big\rangle_T + \big\langle\mathcal{O}^{\tau=4,s=2}\big\rangle_T\,, \quad (11)$$

where $\big\langle\mathcal{O}^{\tau=2,s=2}\big\rangle_T$, $\big\langle\mathcal{O}^{\tau=2,s=4}\big\rangle_T$, and $\big\langle\mathcal{O}^{\tau=4,s=2}\big\rangle_T$ are the twist-2 spin-2, twist-2 spin-4, and twist-4 spin-2 condensates, respectively. A full discussion of these and other non-scalar condensates can be found, e.g., in Refs. [19, 27].

For a consistent implementation of the chirally mixed spectral functions, we need to obtain the leading-order temperature dependence of the condensates. To do so, we must introduce a small parameter about which we are expanding. In the current setup, there are three scales, m_π, T, and Λ_χ, where the latter corresponds to a typical hadronic energy scale (also representing the condensates). At low temperature and small pion mass, there are thus two small ratios available, m_π/Λ_χ and T/Λ_χ. For the temperatures in which we are interested, $m_\pi \sim T$ are of similar size. We define a parameter

$$\lambda \sim \frac{m_\pi}{\Lambda_\chi}, \frac{T}{\Lambda_\chi}, \quad (12)$$

to represent both ratios. Thereby we will work to leading order in λ.

The temperature dependence of a generic operator, $\mathcal{O}$, can be expressed in terms of its vacuum value plus its expectation value within external hadronic states. The matrix elements with single-pion states provide the dominant contribution at low temperatures; thus the temperature dependence can be written as

$$\langle\mathcal{O}\rangle_T \simeq \langle\mathcal{O}\rangle_0 + 3\int\frac{d^3k}{(2\pi)^3\,2E_k}f^\pi(E_k;T)\,\langle\pi^a(\vec{k})|\mathcal{O}|\pi^a(\vec{k})\rangle \quad (13)$$

where f^π denotes the thermal Bose distribution and $E_k = \sqrt{k_\pi^2 + m_\pi^2}$ the pion energy. Soft pion theorems can then be applied so that $\langle\pi^a(\vec{k})|\mathcal{O}|\pi^a(\vec{k})\rangle$ becomes momentum independent for scalar operators [19]*. Corrections to the soft pion theorems are suppressed by at least one power of λ. Therefore the entire temperature dependence is contained in the quantity (adopting standard notation)

$$\epsilon(T) = \frac{2}{f_\pi^2}\int_0^\infty\frac{1}{(2\pi)^3}\frac{\mathrm{d}^3p}{E_p}\,f^\pi(E_p;T)\,. \quad (14)$$

The function $\epsilon(T)$ is proportional to the scalar pion density, such that $\epsilon \propto \rho_\pi^s/f_\pi^2$ represents a small parameter. Formally it is $\mathcal{O}(\lambda^2)$, thus the leading finite temperature effects to the condensates are of this order. In the chiral limit, $m_\pi = 0$, it simplifies to $\epsilon(T) = T^2/6f_\pi^2$; however, for finite pion mass, we should evaluate the full expression in Eq. (14).

To find the leading temperature dependence of an operator thus amounts to evaluating the matrix element $\langle\pi^a|\mathcal{O}|\pi^a\rangle$. For quark and gluon condensates to order λ^2 it was derived in Ref. [19],

$$\langle\bar{q}q\rangle_T = \langle\bar{q}q\rangle_0\left(1 - \frac{3}{4}\epsilon(T)\right), \quad (15)$$

$$\left\langle\frac{\alpha_s}{\pi}G_{\mu\nu}^2\right\rangle_T = \left\langle\frac{\alpha_s}{\pi}G_{\mu\nu}^2\right\rangle_0 - \frac{2}{3}m_\pi^2 f_\pi^2\epsilon(T)\,. \quad (16)$$

The leading temperature dependence of the quark condensate has also been derived in Ref. [28], starting from a calculation of the pressure of a low-temperature gas of finite-mass pions to order T^8. The contribution from single-pion states then determines the leading-order temperature dependence of the quark and gluon condensates, which we have verified to match those found in Ref. [19] (note that for finite pion mass, the leading T dependence of the gluon condensate enters at T^4, while for massless pions it comes in at T^8). The temperature dependence of the four-quark condensates was also found in Ref. [19] for $\kappa = 1$. Upon expressing their vacuum values with $\kappa_{V,A} \neq 1$, one obtains

$$\left\langle\mathcal{O}_4^V\right\rangle_T = \kappa_V\,\langle\bar{q}q\rangle_0^2\left(1 - \frac{18}{7}\frac{\kappa}{\kappa_V}\epsilon(T)\right), \quad (17)$$

$$\left\langle\mathcal{O}_4^A\right\rangle_T = \kappa_A\,\langle\bar{q}q\rangle_0^2\left(1 - \frac{18}{11}\frac{\kappa}{\kappa_A}\epsilon(T)\right). \quad (18)$$

We note [12, 18, 19, 29] that factorization of the 4-quark condensate is not expected to hold at finite temperature; the appearance of $\kappa_{V/A}$ in the above expressions is a mere relic of the parametrization in the vacuum. The temperature dependence of the nonscalar operators (again to order λ^2) is given by [19, 21, 27]

$$\big\langle\mathcal{O}^{\tau=2,s=2}\big\rangle_T = A_2^\pi\left(\frac{3}{4}m_\pi^2 I_1(T) + I_2(T)\right), \quad (19)$$

$$\big\langle\mathcal{O}^{\tau=2,s=4}\big\rangle_T = -A_4^\pi\left(\frac{5}{8}m_\pi^4 I_1(T) + \frac{5}{2}m_\pi^2 I_2(T) + 2I_3(T)\right), \quad (20)$$

$$\big\langle\mathcal{O}^{\tau=4,s=2}\big\rangle_T = -B_2^\pi\left(\frac{3}{4}m_\pi^2 I_1(T) + I_2(T)\right), \quad (21)$$

* Nonscalar operators can still depend on the pion momentum because of their spin structure. However, the dependence is usually simple enough that the integral over momentum can still be performed.

where

$$I_n(T) = \int_0^\infty \frac{\mathrm{d}^3p}{(2\pi)^3}\frac{(p^2)^{n-1}}{E_p}\, f^\pi(E_p;T)\ . \qquad (22)$$

Note that $I_1(T) = f_\pi^2\epsilon(T)/2$. The quantities A_2^π and A_4^π represent moments of the light-quark distribution functions, $\psi(x,\mu^2)$, inside the pion as

$$A_n = 2\int_0^1 dx\, x^{n-1}\left[\psi(x,\mu^2) + \bar\psi(x,\mu^2)\right]. \qquad (23)$$

Following Refs. [19, 30], we will use $A_2^\pi = 0.97$ and $A_4^\pi = 0.255$. The parameter B_2^π can be determined from deep inelastic scattering, which in the case of the nucleon gives $B_2^N = -0.247\mathrm{GeV}^2$. A similar measurement for the pion is not available. Therefore we will proceed by taking $B_2^\pi = 0$ and assessing deviations from this value as part of the uncertainty in our calculations.

Since we will need to numerically evaluate the QCDSRs, a metric is needed to quantify the agreement of the two sides of a given QCDSR. We use the method proposed by Leinweber [31] which constructs the average deviation between the left-hand side (LHS) and right-hand side (RHS) of the sum rule over a range of $\mathcal{M}^2$[†]. This measure, known as the d value [31, 32], is defined by

$$d \equiv \frac{1}{\Delta\mathcal{M}^2}\int_{\mathcal{M}^2_{\rm min}}^{\mathcal{M}^2_{\rm max}}\left|1 - \frac{\rm LHS}{\rm RHS}\right|\mathrm{d}\mathcal{M}^2. \qquad (24)$$

The Borel-mass window, within which the sum rule is expected to be valid, is bound by $\mathcal{M}^2_{\rm max}$ and $\mathcal{M}^2_{\rm min}$. The size of the window is given by $\Delta\mathcal{M}^2 = \mathcal{M}^2_{\rm max} - \mathcal{M}^2_{\rm min}$. The lower end of the window, $\mathcal{M}^2_{\rm min}$, is determined such that the contribution of the c_3 term in the QCDSR has reached 10% of the OPE side. The upper end, $\mathcal{M}^2_{\rm max}$, is found so that the continuum contribution to the LHS of the QCDSR has reached half of the contribution from the resonances. This definition is slightly different than what has been used in Refs. [31, 32] due to the larger continuum threshold in the spectral functions used here, but the resulting Borel window is comparable in size to those of the previous works.

C. Finite temperature Weinberg-type sum rules

The extension of the WSRs to finite temperatures was systematically investigated in Ref. [12]. Corresponding expressions for WSR-1 and -2 were obtained while also deriving both the vacuum and finite-temperature forms of WSR-3. We are unaware of any finite-temperature analogue to WSR-0. For mesons at rest in the heat-bath frame (i.e., for vanishing three-momentum), the in-medium WSRs simplify to

$$\int_0^\infty \frac{\Delta\bar\rho(s,T)}{s}\,\mathrm{d}s \;=\; 0, \qquad (25)$$

$$\int_0^\infty \Delta\bar\rho(s,T)\,\mathrm{d}s \;=\; 0, \qquad (26)$$

$$\int_0^\infty \Delta\bar\rho(s,T)\,s\,\mathrm{d}s \;=\; -2\pi\alpha_s\left\langle\mathcal{O}_4^{SB}\right\rangle_T. \qquad (27)$$

As above, we use the notation $\Delta\bar\rho \equiv \rho_V - \bar\rho_A$ to include the pion pole in the axial-vector spectral function.[‡] This is to account for the pion developing a nontrivial self-energy in medium. The temperature dependence of $\left\langle\mathcal{O}_4^{SB}\right\rangle$ was established in Refs. [12, 18] as

$$\left\langle\mathcal{O}_4^{SB}\right\rangle_T = \left\langle\mathcal{O}_4^{SB}\right\rangle_0\left[1 - 2\epsilon(T)\right]. \qquad (28)$$

III. FINITE-TEMPERATURE SPECTRAL FUNCTIONS

A main ingredient to the present work is the model-independent leading-order temperature result for vector and axial-vector spectral functions. In Ref. [13] it was shown that in a dilute pion gas a vector current interacts with thermal pions to produce an axial-vector current and vice versa. The in-medium vector and axial-vector spectral functions then become linear combinations of the vacuum spectral functions,

$$\rho_V(s,T) \;=\; [1-\epsilon(T)]\;\rho_V(s,0) + \epsilon(T)\,\bar\rho_A(s,0)\ , \qquad (29)$$

$$\bar\rho_A(s,T) \;=\; [1-\epsilon(T)]\;\bar\rho_A(s,0) + \epsilon(T)\,\rho_V(s,0)\ . \qquad (30)$$

One can derive these relations in the same way as the temperature dependence of the operators were determined through an expression analogous to Eq. (13). Corrections are therefore likewise suppressed by λ. The temperature dependence is also determined by the same parameter $\epsilon(T)$ given by Eq. (14). In the context of the spectral functions, $\epsilon(T)$ takes on the role of a "mixing parameter" between the vector and axial-vector channels. Extrapolating the mixing prescription to high temperatures yields degenerate spectral functions for $\epsilon = 1/2$. Since the above expressions are based on low-energy effective theory (current algebra), it is implied that one should mix only the non-perturbative regions of the spectral functions and leave the perturbative contributions unaltered.

Since the above mixing procedure only relies on vacuum spectral functions, the agreement of those with vacuum sum rules is essential. Here we employ the vector and axial-vector spectral functions of Ref. [24], which

[†] In this definition, the continuum contribution to the spectral functions is moved to the RHS of each sum rule.

[‡] The vacuum sum rules can also be expressed in terms of $\bar\rho_A$, yielding the same structure as Eqs. (25)-(27) but with $\left\langle\mathcal{O}_4^{SB}\right\rangle$ evaluated in vacuum.

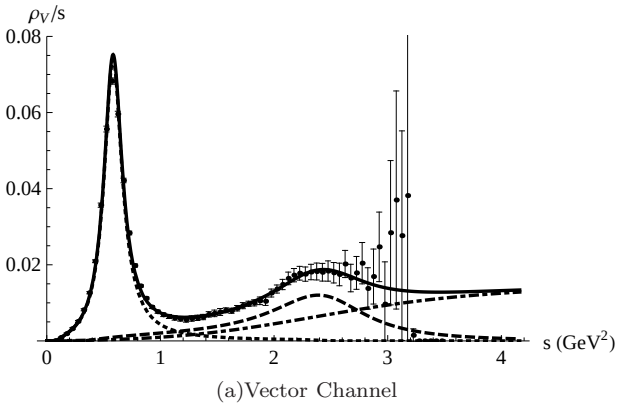

(a)Vector Channel

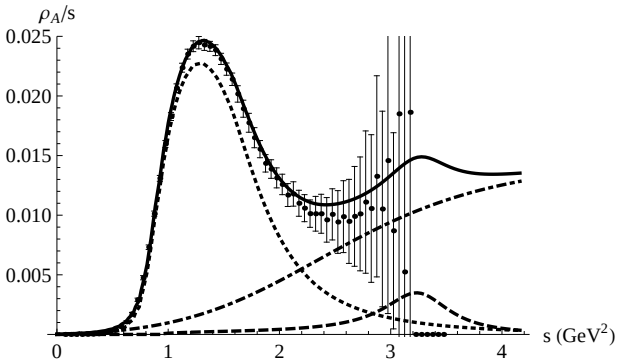

(b)Axial-Vector Channel

FIG. 1: Vacuum spectral functions from Ref. [24] compared with ALEPH τ-decay data [25]. The contributions to the total spectral function (solid lines) are due to the ground-state resonance (dotted curve), excited resonance (dashed curve) and a universal continuum (dotted-dashed curve).

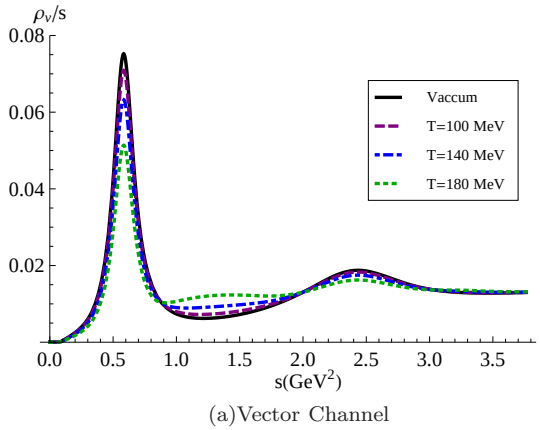

(a)Vector Channel

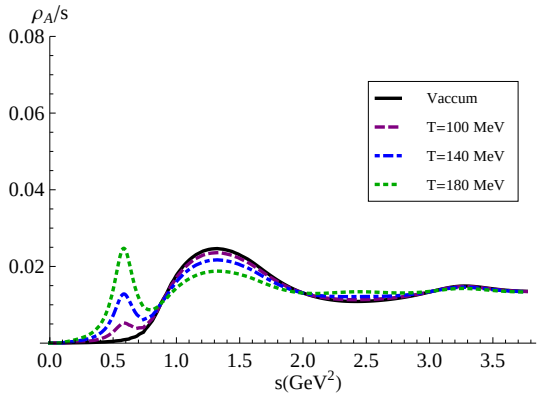

(b)Axial-Vector Channel

FIG. 2: (Finite-temperature vector and axial-vector spectral functions as following from the chiral mixing of the vacuum ones of Fig. 1.

each contain a ground-state resonance, an excited resonance, and a smooth degenerate continuum. These spectral functions were constructed to agree with ALEPH τ-decay data [25] and further constrained by the WSRs. Near-perfect agreement was achieved for WSR-1 and -2, while WSR-0 deviated by -1.28% and WSR-3 by -96% (the latter is actually rather small on the scale of the oscillations over the nonperturbative integration regime). The negative sign in the deviations indicates the axial-vector channel's contribution to be larger. In most previous data-based analyses of the WSRs [25, 26, 33], the energy integration was terminated at the τ mass. In Ref. [24] a convergence of the sum rules was established by going beyond this limit, which dictated the introduction of an $a_1'(1800)$ state as one of the novel features in that work. In addition, agreement with the vacuum QCDSRs was found by using $\alpha_s(1\ \text{GeV}^2) = 0.5$ and optimizing parameter values to find $\langle \frac{\alpha_s}{\pi} G_{\mu\nu}^2 \rangle = 0.022$ GeV^4 and $\kappa_V = \kappa_A = 2.1$, resulting in deviations of $d_V = 0.24\%$ and $d_A = 0.56\%$ over the Borel windows of 0.085 GeV $< \mathcal{M} <$ 1.47 GeV for the vector and 0.089 GeV $< \mathcal{M} <$ 1.48 GeV for the axial-vector channel, respectively.[§]

The resulting vacuum spectral functions, displayed in Fig. 1, contain several key features. The inclusion of excited states in both channels moves the continuum to higher energies while maintaining (or even improving) agreement with the τ-decay data. The different masses of the excited vector and axial-vector states (ρ' and a_1') imply chiral symmetry to be still broken in this energy region. Consequently, the perturbative regime commences at higher energies with degenerate continua in the two channels [24], thus consistently delineating perturbative and nonperturbative components.

The leading-order finite-temperature spectral functions now follow by mixing the nonperturbative parts

[§] The value of α_s was chosen in accordance with previous works and to match the energy scale of the vacuum Borel window, which is centered around 1 GeV^2. Smaller values of α_s were explored, all yielding significantly larger d values. Our best-fit value for the gluon condensate (verified independently of Ref. [24]) turns out to be somewhat larger than the values inferred in Ref. [2], but is not incompatible with other recent works in the literature, see, e.g., the discussion in Ref. [34].

of the vacuum spectral functions via Eqs. (29) and (30), cf. Fig. 2. Note that there is no issue of mixing continua with different thresholds, or perturbative with nonperturbative parts. Chiral mixing induces a mutual flattening of the oscillatory pattern of "peaks" and "valleys" in the vacuum spectral functions, with the peaks in one channel filling in the valleys in the opposite channel: the valley between the ρ and ρ' is filled by the a_1 peak while the valley between the a_1 and a_1' is filled by the ρ' peak, while the spectral strength in the peaks is suppressed.

IV. IN-MEDIUM SUM-RULE ANALYSIS

In this section, we implement the finite-temperature spectral functions derived from chiral mixing into the WSRs (Sec. IV A) and QCDSRs (Sec. IV B), followed by a brief discussion (Sec. IV C).

A. Weinberg sum rules

The in-medium WSRs, Eqs. (25)-(27), depend on the difference of the vector and axial-vector spectral functions, $\Delta\bar{\rho}$. Using chiral mixing, Eqs. (29) and (30), one has

$$\begin{aligned}\Delta\bar{\rho}(s,T) &= \rho_V(s,T) - \bar{\rho}_A(s,T) \\ &= [1-2\epsilon(T)]\,\Delta\bar{\rho}(s,0)\ .\end{aligned} \tag{31}$$

Thus the in-medium WSR-1 and -2 remain intact provided their vacuum limit is satisfied (in fact, residual deviations in the vacuum are suppressed toward chiral restoration). Since the leading-temperature dependence of the four-quark condensate is given by $(1-2\epsilon)$, WSR-3 is also satisfied by the chirally mixed spectral functions. This result holds for any vacuum spectral function provided that no further adjustments are applied, e.g., in the treatment of the continua [12].

B. QCD sum rules

Let us begin by revisiting the QCDSRs in the massless-pion limit of the chiral-mixing scenario. One has $\epsilon = T^2/6f_\pi^2$ so that the leading temperature dependence is of order T^2. Both sides of the sum rule can then be expanded to this order. The LHS takes the form

$$\begin{aligned}&\frac{1}{\mathcal{M}^2}\int\frac{\rho_V(s,0)}{s}e^{-s/\mathcal{M}^2} \\ &\quad+\epsilon(T)\frac{1}{\mathcal{M}^2}\int\frac{\bar{\rho}_A(s,0)-\rho_V(s,0)}{s}e^{-s/\mathcal{M}^2}.\end{aligned} \tag{32}$$

The second integral can be evaluated using the vacuum QCDSRs. Because it reflects the difference between the axial-vector and vector spectral functions, the only term that survives is the chirally breaking 4-quark condensate; thus

$$\text{LHS} = \frac{1}{\mathcal{M}^2}\int\frac{\rho_V(s,0)}{s}e^{-s/\mathcal{M}^2} + \frac{\epsilon(T)}{\mathcal{M}^6}\pi\alpha_s\left\langle\mathcal{O}_4^{SB}\right\rangle. \tag{33}$$

For the RHS (OPE side), the vanishing pion mass makes the quark-condensate term and the temperature correction to the gluon condensate vanish, while the non-scalar terms are higher powers of T^2 compared with $\epsilon(T)$. The terms that remain are the c_0 term, the gluon condensate, and the vector 4-quark condensate along with its temperature dependence. Upon expanding the c_3 term, the temperature corrections to the vector 4-quark condensate can be written in terms of the chirally breaking 4-quark condensate,

$$-\frac{56}{81}\pi\alpha_s\left\langle\mathcal{O}_4^V\right\rangle_T = -\frac{56}{81}\pi\alpha_s\left\langle\mathcal{O}_4^V\right\rangle + \epsilon(T)\pi\alpha_s\left\langle\mathcal{O}_4^{SB}\right\rangle. \tag{34}$$

Thus the RHS takes the form

$$\begin{aligned}\text{RHS} = c_0 &+ \frac{1}{24\mathcal{M}^4}\left\langle\frac{\alpha_s}{\pi}G_{\mu\nu}^2\right\rangle \\ &+ \frac{1}{\mathcal{M}^6}\left(-\frac{56}{81}\pi\alpha_s\left\langle\mathcal{O}_4^V\right\rangle + \epsilon(T)\pi\alpha_s\left\langle\mathcal{O}_4^{SB}\right\rangle\right).\end{aligned} \tag{35}$$

Comparing the LHS and RHS of the QCDSRs one now sees that the chirally breaking 4-quark condensate cancels between the two sides while the remaining terms are simply the vector QCDSR in vacuum. A similar derivation can be made for the axial-vector channel as well. Thus, for massless pions, the QCDSRs are analytically satisfied to order ϵ (see also Ref. [22]).

However, for finite pion mass, some of the simplifications on the OPE side no longer occur. The expressions for the LHS remain unchanged, while the temperature dependence of the vector 4-quark condensate still can be expressed in turns of the chirally breaking 4-quark condensate so that the cancelation between the two sides for this term occurs. However, terms which vanished or were temperature suppressed are now present, involving factors of the squared pion mass. Most notably, there is an incomplete cancelation between the temperature corrections of the quark condensate, the gluon condensate, and the twist-2, spin-2 condensates. A similar lack of cancelation applies to the dimension-6 nonscalar operators. The balance of these partial cancelations produces terms on the RHS which are order λ^2 where there are no such terms on the LHS. Thus the QCDSRs are explicitly violated at order λ^2. Therefore we must proceed by numerically evaluating the QCDSRs to determine to what degree quantitative deviations affect the validity of the mixing scheme at a given temperature.

The two sides of each channel's sum rule are displayed in Fig. 3 for four different temperatures as a function of Borel mass, while Table I quantifies the average deviation, Eq. (24), over the pertinent in-medium Borel window. Since neither channel's vacuum spectral functions exactly satisfy the vacuum QCDSRs, residual vac-

T (MeV)	0	100	110	120	130	140	150	160	170	180
ϵ	0	0.06	0.08	0.10	0.13	0.16	0.20	0.23	0.28	0.32
d_V(%)	0.24	0.32(0.29)	0.38(0.33)	0.48(0.39)	0.64(0.51)	0.85(0.64)	1.11(0.74)	1.43(0.97)	1.82(1.17)	2.29(1.39)
d_A(%)	0.56	0.65(0.57)	0.70(0.58)	0.78(0.61)	0.90(0.67)	1.08(0.76)	1.30(0.88)	1.60(1.01)	1.98(1.17)	2.53(1.34)

TABLE I: Average deviation of the QCDSRs over the Borel window for the vector and axial-vector channels at select temperatures. Values in parentheses are based on a frozen Borel window identical to the vacuum one.

uum deviations will contribute to the in-medium analysis. Therefore it is important to compare the in-medium deviations with the vacuum's deviation. Overall, the d values stay within a factor of two of the vacuum values for temperatures up to 120-140 MeV for the vector and axial-vector channels, respectively. These temperatures also roughly reflect the range within which the d values are approximately linear in ϵ, as one would expect in the regime of validity. Thus one may conclude that the QCDSRs are reasonably well satisfied up to these temperatures.

Let us address some of the uncertainties in the evaluation of the QCDSRs. Closer inspection of the Borel window reveals its lower end to expand significantly with temperature, see Fig. 3. The decrease of $\mathcal{M}^2_{\rm min}(T)$ can be attributed to the decrease of the c_3 term with T, i.e., the 10%-level contribution of the $1/\mathcal{M}^6$ moves to lower $\mathcal{M}^2$. In fact, the low-end portion of the Borel window (extending outside the vacuum window) causes most of the increase of the deviation at higher temperature. If instead one postulates the in-medium Borel window to be the same as in vacuum (indicated by the vertical lines in Fig. 3), the d values decrease appreciably at higher temperatures (quoted in parenthesis in Table I), thus staying within a 1% margin up to temperatures as high as 160 MeV.

Further uncertainties are due to the non-scalar terms in the in-medium OPE. The accuracy of the twist-2 contributions, A_2^π and A_4^π, is not well known, while B_2^π has not been measured for the pion. We find the impact of the twist-2 terms on the d values to be small, while B_2^π produces a more significant deviation. For example, a 20% change in the value of A_2^π causes a *relative* change of less than 0.7% in d_V and d_A for all temperatures. A similar variation in A_4^π causes a larger relative deviation in d_V and d_A of $\sim 5\%$ at the higher temperatures, but less than 0.1% at the lowest temperature. A larger uncertainty arises from the numerical value of B_2^π. While this parameter has not been experimentally measured for the pion, a relative estimate of its size may be made by adopting the value for the nucleon, $B_2^N = -0.247{\rm GeV}^2$. We then find that d_V is altered by less than 1% at 100 MeV but as much as 25% at 180 MeV. The effect on the axial-vector channel is not as pronounced with the maximum relative deviation of 5% at the highest temperature.

C. Discussion

Let us finally put our results into context with previous works on in-medium sum rules. Most QCDSR analyses thus far have been based on a ground-state plus continuum ansatz for the vector and/or axial-vector spectral function. This usually implied that (a) the continua in the two channels are different, and (b) a reduction of the in-medium threshold was deduced from the QCDSRs. Both properties can potentially cause complications when carried out within a rigorous low-temperature implementation as given by chiral mixing, due to overlaps of the nonperturbative resonance regime with the perturbative continuum in the two channels. This becomes particularly problematic in the WSRs, whose low-temperature versions require a strict mixing of the entire vacuum spectral functions. In the present work, we resolve this issue by employing vacuum spectral functions with a universal separation of nonperturbative and perturbative regimes, thanks to excited states and a degenerate continuum. This ensures a straightforward fulfillment of the low-temperature WSRs (i.e., within chiral mixing) but also maintains a numerical agreement of the QCDSRs in both vector and axial-vector channels at low temperature.

The WSRs and the QCDSRs for chirally mixed axial-/vector spectral functions are analytically satisfied in the chiral limit, without an apparent limitation due to temperature for their validity. However, for finite pion mass, the QCDSR are violated at order λ^2. The then-required numerical evaluation of the QCDSRs does exhibit deviations suggesting their breakdown at temperatures of the order of the pion mass. It is interesting that this breakdown roughly sets in at temperatures where one expects corrections from higher resonances to become important. This is not seen if only massless pions are considered.

V. CONCLUSIONS

In the present work we have performed a simultaneous analysis of QCD and Weinberg-type sum rules with vector and axial-vector spectral functions in the low-temperature limit. Specifically, we have utilized updated vacuum spectral functions as an ingredient to their chiral mixing, and numerically evaluated the role of pion mass corrections in the sum rules. The in-medium spectral functions confirm earlier findings of a mutual flatten-

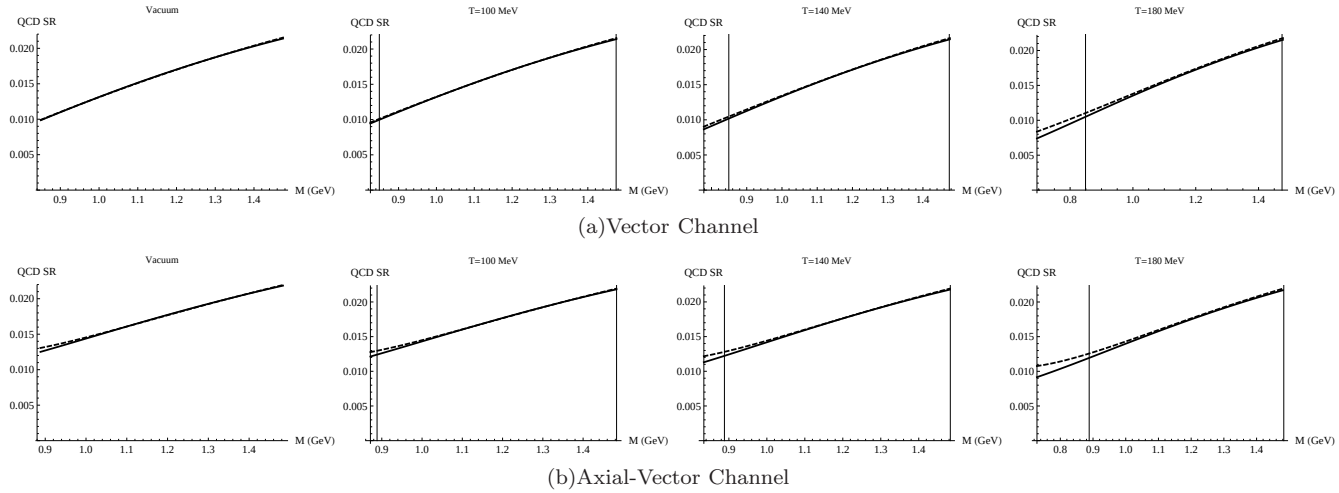

(a)Vector Channel

(b)Axial-Vector Channel

FIG. 3: Comparison of the LHS (solid curve) and RHS (dashed curve) of the QCDSRs the vector (upper panels) and axial-vector (lower panels) channels at select temperatures. The extent of each plot corresponds to the Borel window at that temperature, while the vertical lines designate the Borel window in vacuum.

ing trend with increasing temperature. While the WSRs could be shown to remain valid analytically (thereby avoiding a mixing of perturbative and nonperturbative components in the spectral functions), the finite pion mass corrections required a numerical analysis of the QCDSRs. They were found to be reasonably satisfied up to temperatures of about 140 MeV, with deviations markedly increasing beyond. This may be an indirect indication for additional physics, beyond low-energy chiral pion dynamics, which is, of course, well known from other contexts (resonance excitations). Our work may be extended to include more realistic medium effects, either by working to higher orders in T/Λ_χ and m_π/Λ_χ, or by considering spectral functions which are known to agree with dilepton emission data. It is instructive to note that even the most simple, yet rigorous, construction of low-temperature vector and axial-vector spectral functions satisfies sum rules rooted in QCD while suggesting a mechanism that could play a role toward their degeneration.

Acknowledgments

The work of N.P.M.H., P.M.H., and R.R. is supported by the US-NSF Grant No. PHY-0969394 and by the A.-v.-Humboldt Foundation (Germany). N.P.M.H. thanks M. Causey for valuable discussions.

[1] E. V. Shuryak, World Sci. Lect. Notes Phys. **71**, 1 (2004).
[2] B.L. Ioffe, V.S. Fadin, and L.N. Lipatov, *Quantum Chromodynamics: Perturbative and Nonperturbative Aspects* (Cambridge University Press, New York, 2010)
[3] Edited by B. Friman, C. Hohne, J. Knoll, S. Leupold, J. Randrup, R. Rapp, and P. Senger, Lect. Notes Phys. **814**, 1 (2011).
[4] H. Satz, Lect. Notes Phys. **841**, 1 (2012).
[5] J. Beringer *et al.* (Particle Data Group), Phys. Rev. D**86**, 010001 (2012).
[6] S. Borsanyi *et al.* (Wuppertal-Budapest Collaboration), J. High Energy Phys. 09 (2010) 073.
[7] A. Bazavov, T. Bhattacharya, M. Cheng, C. DeTar, H. T. Ding, S. Gottlieb, R. Gupta and P. Hegde *et al.*, Phys. Rev. D **85**, 054503 (2012).
[8] M. A. Shifman, A. I. Vainshtein and V. I. Zakharov, Nucl. Phys. **B147**, 385 (1979).
[9] M. A. Shifman, A. I. Vainshtein and V. I. Zakharov, Nucl. Phys. **B147**, 448 (1979).
[10] T. Das, V. S. Mathur and S. Okubo, Phys. Rev. Lett. **19**, 859 (1967).
[11] S. Weinberg, Phys. Rev. Lett. **18**, 507 (1967).
[12] J. I. Kapusta and E. V. Shuryak, Phys. Rev. D **49**, 4694 (1994).
[13] M. Dey, V. L. Eletsky and B. L. Ioffe, Phys. Lett. B **252**, 620 (1990).
[14] J. V. Steele, H. Yamagishi and I. Zahed, Phys. Lett. B **384**, 255 (1996).
[15] G. Chanfray, J. Delorme and M. Ericson, Nucl. Phys. **A637**, 421 (1998).
[16] B. Krippa, Phys. Lett. B **427**, 13 (1998).
[17] M. Harada, C. Sasaki and W. Weise, Phys. Rev. D **78**, 114003 (2008).
[18] V. L. Eletsky, Phys. Lett. B **299**, 111 (1993).
[19] T. Hatsuda, Y. Koike and S. -H. Lee, Nucl. Phys. **B394**, 221 (1993).
[20] R. Hofmann, T. Gutsche and A. Faessler, Eur. Phys. J.

C **17**, 651 (2000).
[21] S. Zschocke, O. P. Pavlenko and B. Kampfer, Eur. Phys. J. A **15**, 529 (2002).
[22] E. Marco, R. Hofmann and W. Weise, Phys. Lett. B **530**, 88 (2002).
[23] Y. Kwon, C. Sasaki and W. Weise, Phys. Rev. C **81**, 065203 (2010).
[24] P.M. Hohler and R. Rapp, Nucl. Phys. **A892**, 58 (2012).
[25] R. Barate *et al.* (ALEPH Collaboration), Eur. Phys. J. C **4**, 409 (1998).
[26] K. Ackerstaff *et al.* (OPAL Collaboration), Eur. Phys. J. C **7**, 571 (1999).
[27] S. Leupold and U. Mosel, Phys. Rev. C **58**, 2939 (1998).
[28] P. Gerber and H. Leutwyler, Nucl. Phys. **B321**, 387 (1989).
[29] S. Leupold, J. Phys. G **32**, 2199 (2006).
[30] S. Zschocke, B. Kampfer, O. P. Pavlenko and G. Wolf, arXiv:nucl-th/0202066.
[31] D. B. Leinweber, Ann. Phys. (NY) **254**, 328 (1997).
[32] S. Leupold, W. Peters, and U. Mosel, Nucl. Phys. **A628**, 311 (1998).
[33] B. L. Ioffe, Usp. Fiz. Nauk **171**, 1273 (2001) [Phys. Usp. **44**, 1211 (2001)].
[34] S. Narison, Phys. Lett. B **706**, 412 (2012).